Electronic Supplementary Material (ESI) for RSC Advances.

Self-assembled MoS_2/rGO Nanocomposites with Tunable UV-IR Absorption

Wei Wang,[*1,2] *Olesya O. Kapitanova,*[3] *Pugazhendi Ilanchezhiyan,*[2] *Sixing Xi,*[1]

Gennady N. Panin,[*2,4] *Dejun Fu,*[5] *Tae Won Kang*[2]

[1] *College of Science, Hebei University of Engineering, Handan 056038, China .*

[2] *Department of Physics, Quantum-Functional Semiconductor Research Center, Nano Information Technology Academy, Dongguk University, 100-715, Seoul, Korea*

[3] *Department of Chemistry, Moscow State University, Leninskie Gory, 1, b.3, 119991, Moscow, Russia*

[4]*Institute for Microelectronics Technology & High Purity Materials, RAS, 142432 Chernogolovka, Moscow district, Russia*

[5]*Key Laboratory of Artificial Micro- and Nano-Materials of Ministry of Education and School of Physics and Technology, Wuhan University, Wuhan 430072, China.*

*E-mail: g_panin@dongguk.edu; panin@iptm.ru (G.N.P), wangwe19872010@163.com (W.W)

Figure S1 shows the SEM images of MoS_2/rGO composites on a SiO_2/Si substrate after annealing for the different TAA/GO ratios: (a) 1:0, (b) 1:1, (c) 1:2 and (d) 1:3. rGO deriving from GO acts as a dispersing platform, efficiently reducing the aggregation of MoS_2 with a decrease of the TAA/GO ratio and forming self-assembled layered MoS_2/rGO structures during the hydrothermal process. The morphology of the annealed structure is slightly different from the morphology of as-grown structure (Fig. 1).

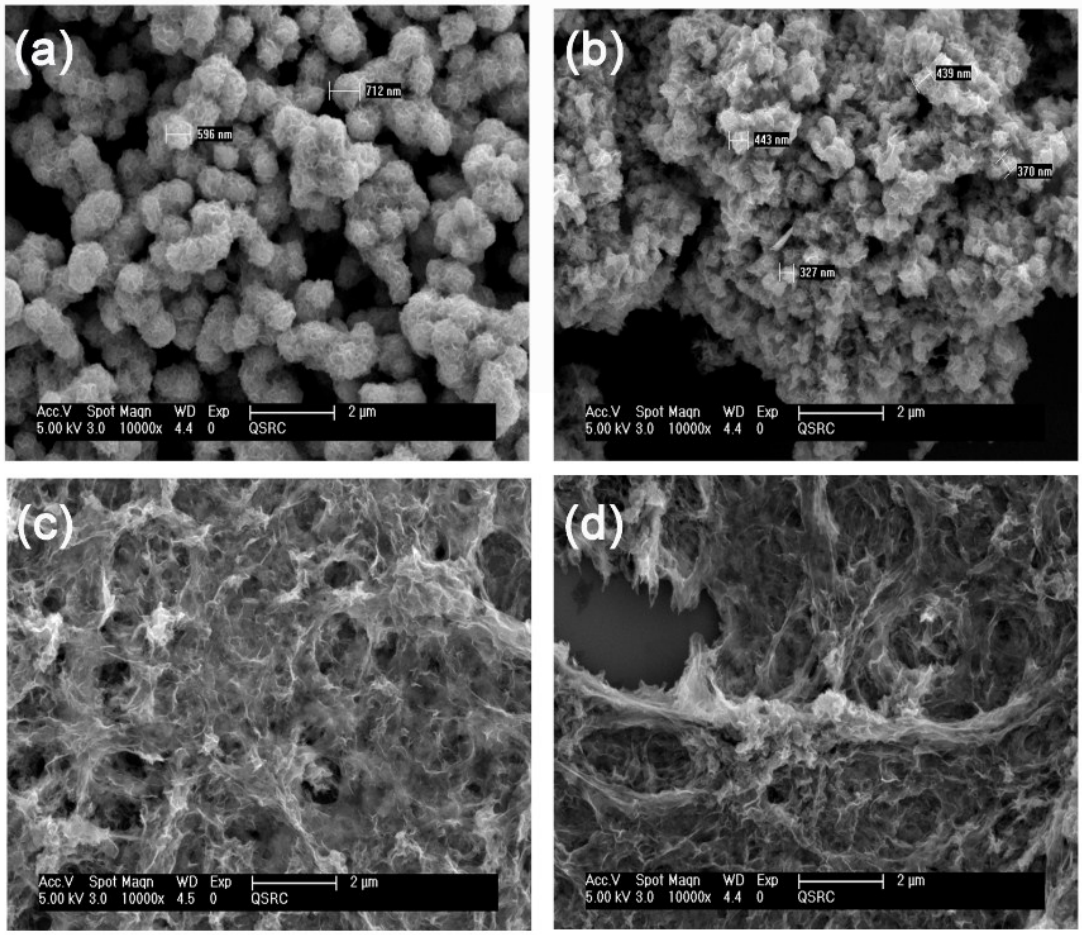

Figure S1. SEM images of MoS_2/rGO composites on a SiO_2/Si substrate after annealing for the different TAA/GO ratios: (a) 1:0, (b) 1:1, (c) 1:2 and (d) 1:3.

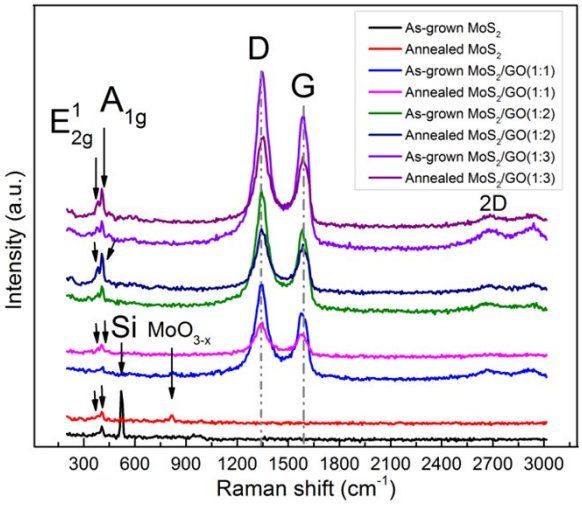

Figure S2. Raman spectra of MoS_2 and MoS_2/rGO composites with different GO content before and after annealing (fitted with Lorentzian functions).

The Raman spectra of MoS_2 (Fig. S2) show the weak peak at 820 cm^{-1} which corresponds to the M=O bending stretch vibrations for MoO_{3-x} and can be ascribed to the formation of molybdenum oxide during annealing process [1-2]. This peak disappeares in the spectra of MoS2/GO composites, indicating a stronger binding of oxygen to carbon. The origin of the main peaks of the MoS_2/r-GO composite (E^1_{2g}, A_{1g} and G, D) is discussed in the description of Fig. 2b. The 520 cm^{-1} peak and the peaks at ~2700 and ~ 2930 cm^{-1} correspond to the Si substrate [3] and the second-order 2D and D+G bands of graphene [4-5], respectively.

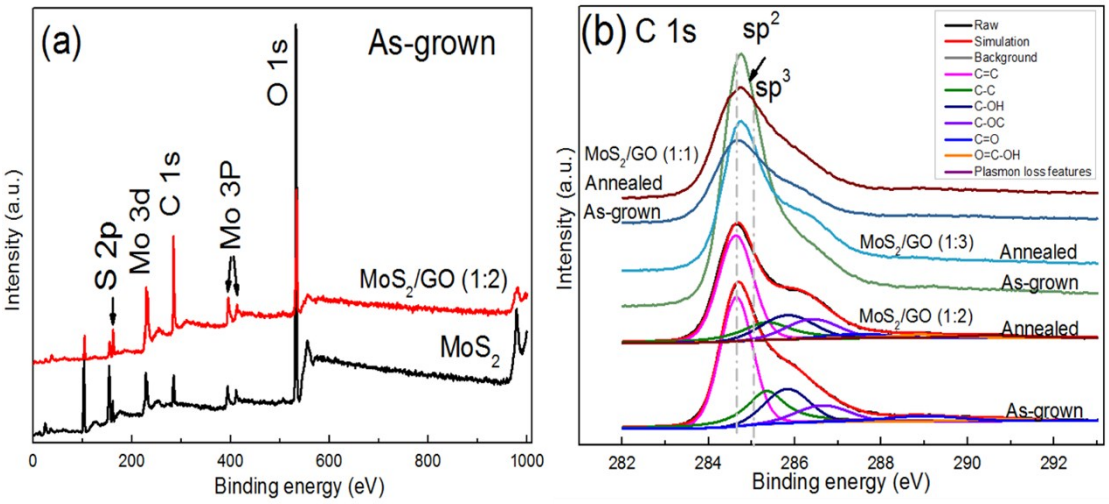

Figure S3. X-ray photoelectron spectra of MoS_2 and MoS_2/rGO composites corresponding to (a) survey, and (b) C 1s core levels.

The chemical composition and binding energies of elements in MoS_2/rGO composites were investigated using XPS. Figure S3 shows the X-ray photoelectron spectra of MoS_2 and MoS_2/rGO composites corresponding to (a) survey, and (b) C 1s core levels. To fit the spectra of composites with MoS_2/GO ratios 1:2 and 1:3, two doublets and splittings of 1.2 and 3.1 eV for S 2p and Mo 3d, respectively, were used. The stronger C 1s signal of the MoS_2/GO (1:2) compared to MoS_2 (Fig. S3a) clearly indicates a significant hydrothermal GO reduction during the synthesis. The low intensity of the Mo 3d signals is apparently due to the formation of $Mo_2S_xO_{1-x}$ and Mo_2S_5, which shows an intermediate product in the MoS_3-to-MoS_2 transition reacting with oxygen from GO deoxygenation. The spectra of C 1s can be decomposed into six components. Peaks at 284.6, 285.3, 285.8, 286.6, 287.5, 288.99 correspond to C=C (sp^2) of 48.1 %, C-C (sp^3) of 20.4 %, C-OH of 16.4 %, C-O-C of 9.5 %, C=O of 1.2 %, and O=C-OH of 4.4 %, respectively, further confirming the existence of rGO in the composites (Fig. S3b).

Table S1. Detailed characteristics of Raman scattering of MoS_2 and MoS_2/rGO composites.

Specimen		Peak position(cm^{-1})		FWHM (cm^{-1})		Peak position(cm^{-1})	
		E^1_{2g}	A_{1g}	E^1_{2g}	A_{1g}	D	G
MoS_2	As-grown	381.2	407.6	35.1	12.8	/	/
	Annealed	381.2	407.4	26.96	12.7	/	/
MoS_2/rGO (1:1)	As-grown	381.9	406.6	30.6	19.9	1342.3	1576.4
	Annealed	382.1	405.3	28.4	17.6	1341.7	1573.98
MoS_2/rGO (1:2)	As-grown	382.1	404.6	22.0	13.6	1345.9	1578.6
	Annealed	382.6	404.5	21.3	15.7	1348.7	1581.4
MoS_2/rGO (1:3)	As-grown	382.6	404.4	17.9	12.1	1347.6	1581.7
	Annealed	382.7	404.1	20.5	15.2	1349.1	1581.9

Table S2. Chemical composition and energy of chemical bonds of components.

Specimen		Chemical Composition (At. %)		Mo $3d_{5/2}$ (eV)			S $2p_{3/2}$ (eV)	
		S	Mo	S-Mo-S	S-Mo-O	O-Mo-O	S-Mo-S	S-Mo-O
MoS_2	As-grown	59.8	40.2	229.4	229.7	233.4	161.4	162.2
	Annealed	67.97	32.1	229.5	230.4	233.3	161.6	162.3
MoS_2/rGO (1:1)	As-grown	58.5	41.5	229.2	229.6	232.6	162.1	162.2
	Annealed	60.3	39.7	229.2	229.7	232.9	162.0	162.4
MoS_2/rGO (1:2)	As-grown	59.8	40.2	229.4	230.6	232.8	162.2	162.7
	Annealed	61.6	38.4	229.3	229.8	232.8	162.1	162.5
MoS_2/rGO (1:3)	As-grown	56.9	43.1	229.5	229.8	232.7	162.3	162.6
	Annealed	64.7	35.3	229.5	231.6	233.2	162.2	162.6

Table S3. Detailed C1s bonds for the MoS_2/rGO (1:2) composite.

Specimen		As-grown MoS_2/rGO (1:2)		Annealed MoS_2/rGO (1:2)	
		Energy (eV)	At.%	Energy (eV)	At.%
Bonding	C=C (sp^2)	284.6	48.1	284.6	48.8
	C-C (sp^3)	285.3	20.4	285.4	15.9
	C-OH	285.8	16.4	285.8	15.8
	C-O-C	286.6	9.5	286.4	12.9
	C=O	287.5	1.2	287.5	3.3
	O=C-OH	289	4.4	288.9	3.3
	Plasmon loss feature	290.9	/	290.5	/

The chemical reaction for the hydrothermal synthesis can be described as:

$$4MoO_4^{2-} + 9CSNH_2^+ + 12H_2O = 4MoS_2 + SO_4^{2-} + 9COOH^+ + 6OH^- + 9NH_3$$

References

[1]B. Yan, Z. Zheng, J.X. Zhang, H. Gong, Z.X. Shen, W. Huang, T.Yu, J. Phys.

Chem. C 113 (2009) 20259-20263.

[2]M. Dieterle, G. Weinberg, G. Mestl, Phys. Chem. Chem. Phys. 4 (2002) 812-821.

[3]M. Baleva, G. Zlateva, A. Atanassov, M. Abrashev, E. Goranova, Phys. Rev. B 72 (2005) 115330-115.

[4]A.C. Ferrari, J.C. Meyer, V. Scardaci, C. Casiraghi, M. Lazzeri, F. Mauri, S. Piscanec, D. Jiang, K.S. Novoselov, S. Roth, A.K. Geim, Phys. Rev. Lett. 97 (2006) 187401-187404.

[5]M.A. Pimenta, G. Dresselhaus, M.S. Dresselhaus, L.A. Cancado, A. Jorio, R. Sato, Phys. Chem. Chem. Phys. 9 (2007) 1276-1291.